Improvement of the accuracy of noise measurements by the two-amplifier correlation method

B. Pellegrini,[1] G. Basso,[1,a)] G. Fiori,[1] M. Macucci,[1] I. A. Maione,[2] and P. Marconcini[1]
[1]*Dipartimento di Ingegneria dell'Informazione, Università di Pisa, via G. Caruso 16, I-56126 Pisa, Italy*
[2]*Institute for Neutron Physics and Reactor Technology (INR), Karlsruhe Institute of Technology (KIT), Campus Nord, Hermann-von-Helmholtz-Platz 1, 76344 Eggenstein-Leopoldshafen, Germany*

(Received 24 June 2013; accepted 16 September 2013; published online 4 October 2013)

We present a novel method for device noise measurement, based on a two-channel cross-correlation technique and a direct "*in situ*" measurement of the transimpedance of the device under test (DUT), which allows improved accuracy with respect to what is available in the literature, in particular when the DUT is a nonlinear device. Detailed analytical expressions for the total residual noise are derived, and an experimental investigation of the increased accuracy provided by the method is performed.
 [http://dx.doi.org/10.1063/1.4823780]

I. INTRODUCTION

Advancements in the field of electron devices, in particular the aggressive downscaling and the progressive exploitation of quantum effects, require the development of measurement techniques with ever-increasing sensitivity. This is particularly challenging in the field of noise measurements, in which no deterministic information about the quantity of interest is available, thereby preventing the application of lock-in or similar techniques to reach a sensitivity below the noise floor of the amplifiers. The preferred approach is represented by correlation techniques,[1–3] which exploit the fact that the useful information appears as correlated signals at the output of two or more[4–6] amplifiers connected to the Device Under Test (DUT), while most of the noise produced by the amplifiers themselves corresponds to uncorrelated contributions, which can be averaged out performing a long enough acquisition of the cross-power spectral density for the different channels. For particular cases, e.g., DUTs with a very large impedance, more complex schemes have been devised for further lowering the undesired noise components.[7]

In order to push the achievable sensitivity of the general two-amplifier correlation technique[1] (valid, with proper circuit choices, over a wide range of DUT impedances) to the limits, we have performed a detailed analytical study of the contributions from the different noise sources in the measurement setup and of their effect on the cross-power spectral density. We specifically focus also on the precise *in situ* evaluation of the transimpedance between the device and the output of the amplifiers, which is essential for a correct determination of the noise characteristics of the device under test, thus extending to correlation measurements a procedure that we had developed for single-amplifier DUT characterization.[8] A direct measurement of the transimpedance by means of a network analyzer or of a similar instrument would not be as accurate, because of the necessity of introducing external connections that would alter the stray capacitances and inductances which exist in the actual measurement setup, and, in the case of strongly nonlinear devices, as a consequence of the fact that small errors in reproducing the bias point may lead to large deviations in the measured transimpedance.

It is also important to point out that the variation of the transimpedance between the DUT and the amplifier output with the bias point is often neglected in the literature and also the contributions from the spurious noise sources do depend on the bias-dependent device impedance, thereby invalidating approaches based on an evaluation of the background noise of the measurement system with the device unbiased. With the technique we propose the transimpedance can be measured easily for each bias condition and then used for an accurate estimation of the DUT noise.

We provide detailed expressions for the total noise at the amplifier outputs, as a function of the various sources and, in particular, we derive an expression for the spurious terms that survive in the cross-power spectral density and validate it by comparison with experimental data that we have obtained from a test setup. Such an expression can be used to establish the ultimate limits of a measurement system based on correlation techniques and provides also an indication of the number of averages (and, therefore, of the total time required) to achieve the maximum sensitivity.

The paper is structured as follows: after this Introduction a short section is devoted to the discussion of the two possible circuit configurations, the "series" and the "parallel" arrangements of the correlation amplifiers; then theoretical results for both configurations are presented, followed by experimental data from actual measurements and conclusions.

II. IMPROVEMENT OF THE ACCURACY IN NOISE MEASUREMENTS

As shown in Ref. 1, cross-correlation techniques allow to increase the sensitivity of the front-end amplifiers used for high-sensitivity noise measurements. Indeed, such a method can almost suppress the effects of the equivalent current (voltage) noise sources I_n (V_n) at the amplifier input when the impedance of the DUT is large (small) compared to that at the amplifier input, and the two independent channels are

a)Electronic mail: g.basso@iet.unipi.it

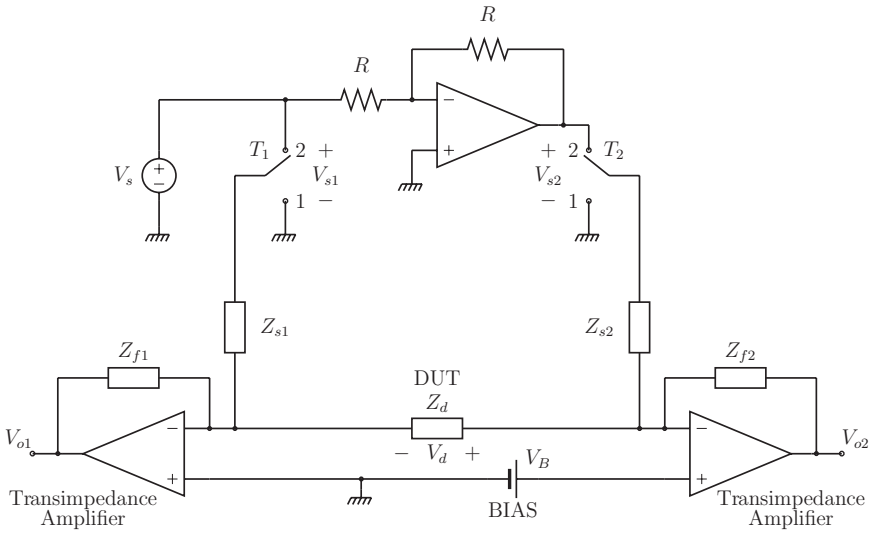

FIG. 1. Schematic diagram of the noise measurement circuit in the improved series configuration. The circuit "in parallel" to the DUT is needed in order to measure the transimpedances between the DUT noise current source and the outputs of the amplifiers.

connected in a "series" ("parallel") configuration, as shown in Fig. 1 (Fig. 2).

The main objective of the present work is, as already stated, the improvement of the accuracy of ultra-low noise measurement systems. This can be achieved by (i) exploiting cross-correlation techniques to minimize the contributions from uncorrelated noise sources; (ii) the direct and accurate measurement of the transimpedance between the equivalent current noise source I_d in parallel to the DUT and the output, thus extending the method proposed for the single channel configuration.[8]

The transimpedance can be evaluated including the impedances Z_{sj} ($j = 1, 2$) (Z_s) and the test voltage sources V_{sj} (V_s), with the switches T_j (T_0) in position 2; during noise measurements, instead, the switches are set in position 1. The detailed calculation of the transimpedance will be presented in the Secs. III and IV. Another objective is represented by the accurate evaluation of the power spectral density of the residual noise due to the correlated noise sources of the two channels, as well as the standard deviation of the fluctuations of the measured noise level after averaging over M independent measurements, fluctuations mainly resulting, for large enough values of M, from uncorrelated noise sources. This is useful to determine the limiting sensitivity achievable by averaging the spectra over a given number of time records or, vice versa, to estimate the number of time records needed to obtain a given sensitivity.

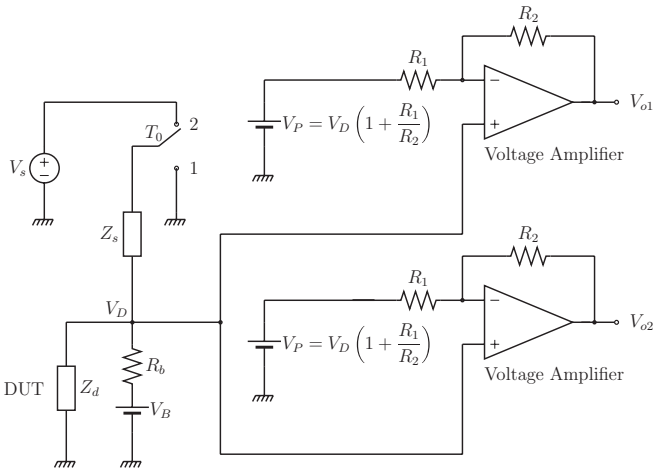

FIG. 2. Schematic diagram of the noise measurement system in the parallel configuration. V_s, Z_s, and the switch T_0 are needed in order to measure the transimpedance between the DUT noise current source and the outputs of the amplifiers.

III. SERIES CONFIGURATION

For large values of the DUT impedance, i.e., much greater than the optimal noise impedance for the amplifier (i.e., the impedance for which the noise figure reaches its minimum value), the achievable sensitivity is limited mainly by the equivalent input current noise sources I_n, whose effects can be reduced with the configuration shown in Fig. 1. In particular, each of the DUT terminals is connected to one of the inputs of the two transimpedance amplifiers, which convert the noise current I_d of the DUT into two output noise voltages V_{o1} and V_{o2}. With this configuration, a bias voltage V_B can be applied to the DUT, too.

In Fig. 3(a), we show one of the transimpedance amplifiers with the associated noise sources (i.e., the equivalent noise sources of the operational amplifier and the thermal noise source I_f of the feedback impedance Z_f), and in Fig. 3(b) we report its equivalent circuit with just two equivalent noise sources at the input port, V_n' and I_n'.

As a result of the shunt-voltage feedback implemented with Z_f, the output impedance of the transresistive amplifier is very small and can be considered to be zero for the present analysis, while the input impedance Z_i is given by $Z_i = Z_{in} \parallel [Z_f/(1 + A_v)]$, (where A_v is the open-loop gain of the operational amplifier) and the voltage gain is simply $A = -A_v$. Since in the presence of a short circuit at the input, the only contribution will be the one from V_n', we can compute

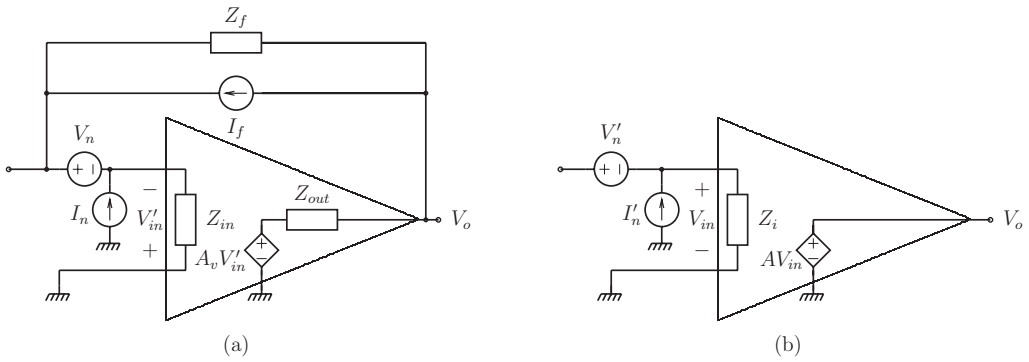

FIG. 3. (a) Schematic diagram of the transresistive amplifier with the indication of all noise sources; (b) equivalent representation of the transresistive amplifier with equivalent voltage and current noise sources at the input port.

its value by placing a short circuit at the input of the amplifiers in Figs. 3(a) and 3(b), evaluating the noise at the output of the circuit in Fig. 3(a), and dividing by the transfer function of the circuit in Fig. 3(b). Therefore $V'_n = V_n$. The evaluation of I'_n can be performed by leaving the input of both amplifiers open, then evaluating the resulting voltage at the output, and dividing it by the transfer function of the circuit in Fig. 3(b). In this way, we obtain $I'_n = I_n - V_n/Z_f + I_f$.

In Fig. 4(a), we report the equivalent schematic diagram of the whole correlation amplifier in the series configuration, where further subscripts have been added to distinguish between the two amplifiers. The current I_j ($j = 1, 2$) is given by

$$I_j = I_{nj} + I_{fj} + I_{sj} + \frac{V_{sj}}{Z_{sj}}, \tag{1}$$

where I_{sj} is the thermal noise source of the impedance Z_{sj}, and V_{sj}/Z_{sj} is the current due to V_{sj} when T_j is set in position 2 and zero otherwise. We notice that the first two terms of the rhs of Eq. (1) correspond to I'_{nj}, except for the term $-V_{nj}/Z_{fj}$, which is separately represented in Fig. 4(a).

Let us now compute the contribution of each of the noise sources of Fig. 4(a) to the output voltages. Due to the symmetry, we perform the calculation only for $j = 2$, noticing that the only difference between the case with $j = 1$ and that with $j = 2$ consists in the sign of the contribution from I_d. In addition, we define $Z_j = Z_{ij} \parallel Z_{sj}$, with reference to the circuits for the calculation of each contribution represented in Figs. 4(b)–4(d). Let us first consider the circuit in Fig. 4(b). The contribution from I_1 to V_{in2} is given by

$$\begin{aligned} V_{in2} &= I_1 \frac{Z_1}{Z_1 + Z_d + Z_2} Z_2 \\ &= \left(I'_{n1} + I_{f1} + I_{s1} + \frac{V_{s1}}{Z_s 1} \right) \frac{Z_1}{Z_1 + Z_d + Z_2} Z_2, \end{aligned} \tag{2}$$

while, from Fig. 4(c), the contribution from I_2 to V_{in2} reads

$$\begin{aligned} V_{in2} &= I_2 (Z_d + Z_1) \parallel Z_2 \\ &= \left(I'_{n2} + I_{f2} + I_{s2} + \frac{V_{s2}}{Z_{s2}} \right) \frac{Z_2 (Z_d + Z_1)}{Z_1 + Z_2 + Z_d} \end{aligned} \tag{3}$$

and the contribution from I_d to V_{in2} (Fig. 4(d)) can be expressed as

$$V_{in2} = -I_d \frac{Z_d Z_2}{Z_d + Z_1 + Z_2}. \tag{4}$$

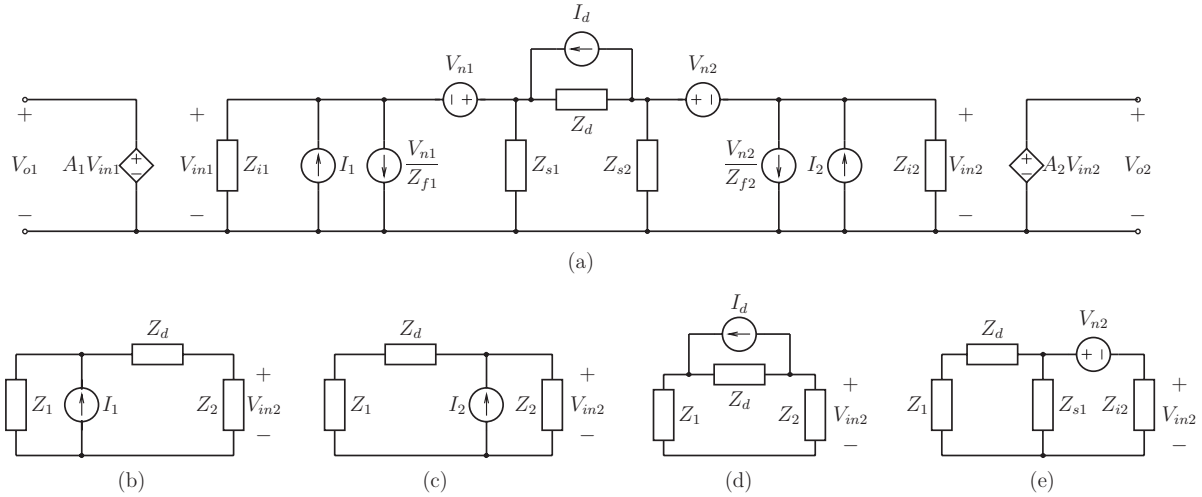

FIG. 4. (a) Equivalent circuit of the measurement system of Fig. 1; (b)–(e) equivalent circuits for the evaluation of the contributions to V_{in2} due to I_1, I_2, I_d, and V_{n2}, respectively.

We can thus write the component V_{oj}^I at the output j, due to just the currents I_1, I_2, and I_d as

$$V_{oj}^I = \frac{Z_d Z_j A_j}{Z_1 + Z_2 + Z_d}\left[(-1)^k I_d + \left(1 + \frac{Z_k}{Z_d}\right) I_j + \frac{Z_k}{Z_d} I_k\right], \tag{5}$$

where $j = 1, 2$, while $k = 2$ for $j = 1$ and $k = 1$ for $j = 2$.

Let us now consider the case with T_j in position 2. Enforcing the conditions $Z_{s1} = Z_{s2} = Z_s$, $V_{s1} = -V_{s2} = V_s$ and choosing the test signal V_s large enough that its current contribution V_s/Z_s overcomes all the noise signals, we have a particular value of I_j that we define

$$\hat{I}_j \simeq (-1)^k \frac{V_s}{Z_s}. \tag{6}$$

Thus, in such a specific situation, the resulting output voltage $\hat{V}_{oj}^I$ due to just the current sources can be written [from Eq. (5)]

$$\hat{V}_{oj}^I \simeq \frac{Z_d Z_j A_j}{Z_1 + Z_2 + Z_d}\left[\left(1 + \frac{Z_k}{Z_d}\right)(-1)^k \frac{V_s}{Z_s} + \frac{Z_k}{Z_d}(-1)^j \frac{V_s}{Z_s}\right]$$
$$= \frac{Z_d Z_j A_j}{Z_s(Z_1 + Z_2 + Z_d)} V_s (-1)^k. \tag{7}$$

Therefore, the transfer function H_j between the test source V_s and the output $\hat{V}_{oj}^I$ reads

$$H_j \equiv \frac{\hat{V}_{oj}^I}{V_s} = (-1)^k \frac{Z_d Z_j A_j}{Z_s(Z_1 + Z_2 + Z_d)} \tag{8}$$

and we can use it to determine the transfer function (transimpedance) between the equivalent noise source in parallel with the DUT, $I_{ej}^I \equiv I_d + (-1)^k[(1 + Z_k/Z_d)I_j + (Z_k/Z_d)I_k]$, and the output. To this purpose, we notice that Eq. (5) can be written

$$V_{oj}^I = Z_s H_j \left\{I_d + (-1)^k \left[\left(1 + \frac{Z_k}{Z_d}\right) I_j + \frac{Z_k}{Z_d} I_k\right]\right\}$$
$$= Z_s H_j I_{ej}^I, \tag{9}$$

where $Z_s H_j$ is the transimpedance between V_{oj}^I and I_{ej}^I, i.e., between the jth output and the equivalent noise current source in parallel with the DUT.

Since the current sources I_j are independent from each other, from Eq. (9) the cross-power spectral density S_{I12}^I of I_{e1}^I and I_{e2}^I can be expressed as (the uncorrelated terms do not contribute to the cross-power spectral density)

$$S_{I12}^I = \frac{S_{12}^I}{|Z_s|^2 (H_1 H_2^*)}$$
$$= S_{I_d} - \frac{Z_1^*}{Z_d^*}\left(1 + \frac{Z_2}{Z_d}\right) S_{I_1} - \frac{Z_2}{Z_d}\left(1 + \frac{Z_1^*}{Z_d^*}\right) S_{I_2}, \tag{10}$$

where S_{12}^I is the cross-power spectral density of the two output voltages V_{o1}^I and V_{o2}^I due only to the current sources, i.e., for $V_{nj} = 0$. The power spectral density S_{I11}^I of I_{e1}^I reads instead

$$S_{I11}^I = \frac{S_{11}^I}{|Z_s H_1|^2} = S_{I_d} + \left|1 + \frac{Z_2}{Z_d}\right|^2 S_{I_1} + \left|\frac{Z_2}{Z_d}\right|^2 S_{I_2}, \tag{11}$$

where S_{11}^I is the power spectral density of the voltage at the output 1 for $V_{nj} = 0$; S_{I_d} is instead the power spectral density of the DUT that we want to measure, and S_{I_j} is the power spectral density associated to I_j.

The configuration we are considering makes sense when the DUT impedance $|Z_d|$ is much greater than $|Z_j|$. In this condition, Eqs. (10) and (11) become

$$S_{I12}^I \simeq S_{I_d} - \frac{Z_1^*}{Z_d^*} S_{I_1} - \frac{Z_2}{Z_d} S_{I_2}, \tag{12}$$

$$S_{I11}^I \simeq S_{I_d} + S_{I_1} \tag{13}$$

and one can notice, comparing the above two equations, that the correlation method introduces two current noise sources (S_{I_1} and S_{I_2}) instead of the single one that would be present with just one amplifier, but the power spectral densities of both of them are suppressed by a factor $|Z_j/Z_d|$ with respect to the value that each source would contribute in the case of single channel amplification [which can be derived from Eq. (11) by setting $S_{I_2} = 0$].

Let us now evaluate the contribution V_{oj}^V to each output associated with the voltage noise sources, which in Fig. 4 are indicated as the result both of the voltage noise sources V_{nj} and the current noise sources V_{nj}/Z_{fj}. As far as the voltage sources V_{nj} are concerned, we can compute their effect $V_{oj}^{V'}$ as follows, based on Fig. 4(e) (relative only to the case $j = 2$, $k = 1$, since the case $j = 1$, $k = 2$ is analogous), taking into account that we have already assumed $|Z_d| \gg |Z_j|$ and adding the hypothesis $|Z_s| \gg |Z_{ij}|$, which, together with the previous assumption, implies also $|Z_d| \gg |Z_{ij}|$:

$$V_{oj}^{V'} = -A_j \frac{Z_{ij}}{Z_{ij} + Z_{sj} \parallel (Z_d + Z_k)} V_{nj}$$
$$+ A_j \frac{Z_{sk}}{Z_{ik} + Z_{sk}} \frac{Z_j}{Z_d + Z_{sk} \parallel Z_{ik}} V_{nk}$$
$$\simeq -A_j \frac{Z_{ij}}{Z_{sj} \parallel Z_d} V_{nj} + A_j \frac{Z_j}{Z_d} V_{nk}$$
$$\simeq \frac{Z_{fj}}{Z_{sj} \parallel Z_d} V_{nj} - \frac{Z_{fj}}{Z_d} V_{nk}. \tag{14}$$

Let us now determine the contribution $V_{oj}^{V''}$ of the current noise sources V_{nj}/Z_{fj}. This can be obtained in a very straightforward way from Eq. (9):

$$V_{oj}^{V''} = Z_s H_j (-1)^j \left[\left(1 + \frac{Z_k}{Z_d}\right) \frac{V_{nj}}{Z_{fj}} + \frac{Z_k}{Z_d} \frac{V_{nk}}{Z_{fk}}\right]. \tag{15}$$

Exploiting the above-mentioned inequalities, we also obtain, from Eq. (8):

$$H_j = (-1)^k \frac{Z_d Z_j A_j}{Z_s(Z_1 + Z_2 + Z_d)}$$
$$\simeq (-1)^k \frac{Z_j A_j}{Z_s} \simeq (-1)^j \frac{Z_{fj}}{Z_{sj}} = (-1)^j \frac{Z_f}{Z_s}, \tag{16}$$

if we consider $Z_{f1} = Z_{f2} = Z_f$ and $Z_{s1} = Z_{s2} = Z_s$.

Thus

$$V_{oj}^{V''} = Z_f \left[\left(1 + \frac{Z_k}{Z_d}\right) \frac{V_{nj}}{Z_f} + \frac{Z_k}{Z_d} \frac{V_{nk}}{Z_f}\right]$$
$$\simeq Z_f \frac{V_{nj}}{Z_f} + Z_f \frac{Z_k}{Z_d} \frac{V_{nk}}{Z_f} \simeq V_{nj} + \frac{Z_k}{Z_d} V_{nk} \simeq V_{nj}. \tag{17}$$

The total contribution V_{oj}^V from the voltage noise sources, from Eqs. (14) and (17), can thus be written

$$V_{oj}^V \equiv V_{oj}^{V'} + V_{oj}^{V''} = \left(1 + \frac{Z_f}{Z_s \parallel Z_d}\right) V_{nj} - \frac{Z_f}{Z_d} V_{nk}. \quad (18)$$

In analogy to what we have done in Eq. (9), and exploiting Eq. (16), we can define an equivalent current source I_{ej}^V in parallel with the DUT that represents the contribution from the voltage noise sources:

$$I_{ej}^V \equiv \frac{V_{oj}^V}{Z_s H_j} = \frac{(-1)^j}{Z_f}\left[\left(1 + \frac{Z_f}{Z_s \parallel Z_d}\right) V_{nj} - \frac{Z_f}{Z_d} V_{nk}\right] = (-1)^j (Y_p V_{nj} - Y_d V_{nk}), \quad (19)$$

where $Y_d = 1/Z_d$, $Y_p = 1/Z_d + 1/Z_s + 1/Z_f$.

Similar to Eqs. (10) and (11), from Eqs. (18) and (16) the contribution of the noise voltages to the power spectral density reads

$$S_{I12}^V = \frac{S_{12}^V}{|Z_s|^2 (H_1 H_2^*)} = Y_d^* Y_p S_{V_1} + Y_d Y_p^* S_{V_2}, \quad (20)$$

$$S_{I11}^V = \frac{S_{11}^V}{|Z_s H_1|^2} = |Y_p|^2 S_{V_1} + |Y_d|^2 S_{V_2}, \quad (21)$$

where S_{12}^V and S_{11}^V are the output power spectral densities evaluated neglecting I_j.

The comparison between Eqs. (20) and (21) shows that, from the point of view of the contribution from the voltage noise sources, the cross-correlation technique does not offer particular advantages with respect to a single-channel system, since $|Y_d|$ and $|Y_p|$ can be of the same order of magnitude, and from Eq. (18) and the schematic in Fig. 1, the effects of V_{nj} at the two outputs are correlated with coefficients close to the amplification of the single channel.

From Eqs. (10), for $|Z_j/Z_d| \ll 1$, and (20), the total cross-spectrum $S_{I12} = S_{I12}^I + S_{I12}^V$ can be expressed as

$$S_{I12} = \frac{S_{12}}{|Z_s|^2 (H_1 H_2^*)} = S_{I_d} - Y_d^* Z_1^* S_{I_1} - Y_d Z_2 S_{I_2} + Y_d^* Y_p S_{V_1} + Y_d Y_p^* S_{V_2}, \quad (22)$$

where $S_{12} = S_{12}^I + S_{12}^V$ is the total cross-power spectral density between the outputs, which can be measured by means of a two-channel Dynamic Signal Analyzer (DSA), that, through its built-in random noise generator V_s, allows the evaluation of H_j, too. In general, dynamic signal analyzers also have the data processing capability to perform all the operations needed to compute the first right-hand term of Eq. (22) and the term $1/|Z_s|^2$. In particular, we assume Z_s to be a capacitor ($1/|Z_s|^2 = (C_s\omega)^2$). This is a convenient choice because its value is relatively constant with frequency (using a low-loss mica capacitor), parasitic capacitances towards other nodes can be neglected (for $C_s > 20$ pF), and there is no contribution in terms of thermal noise ($I_{sj} = 0$), as long as dissipative losses can be neglected; the only drawback being represented by a reduction of the bandwidth, as it will be shown in the following.

The considered circuit allows to directly obtain the module and the real and imaginary parts of S_{I12} and S_{I11}, from which one can evaluate S_{I_d}.

Since two operational amplifiers (OPAMPs) fabricated on the same chip can be used, we consider the same parameters for the two of them, including the noise sources and the input impedances, so that $S_{V_1} = S_{V_2} = S_V$, $S_{I_1} = S_{I_2} = S_I$, $Z_1 = Z_2 = Z$.

As a consequence, in the case of perfect symmetry, from Eq. (22) we would obtain $\mathrm{Im}\{S_{12}^I\} = 0$ and therefore

$$S_{I12} = S_{I_d} + S_r, \quad (23)$$

where, defining $U_I = -2\mathrm{Re}\{Y_d Z\}$ and $U_V = 2\mathrm{Re}\{Y_d Y_p\}$, we can write the residual correlated (and therefore unavoidable) component S_r as

$$S_r = U_I S_I + U_V S_V, \quad (24)$$

where we have $1/R_p = 1/R_d + 1/R_f + 1/R_s$, $C_p = C_d + C_f + C_s$ and finally

$$U_V = \frac{2}{R_p R_d} + 2C_d C_p \omega^2 = \frac{2}{R_d^2}\left(1 + \frac{R_d}{R_f}\right) + 2C_d C_p \omega^2. \quad (25)$$

In practice this is only an approximation, because there will always be tiny differences between the two channels, which will give rise to a nonzero imaginary part of the cross-power spectral density. Indeed, the ratio of the modulus of the imaginary part to that of the real part of the cross-power spectral density can be used as an indication of the degree of symmetry of the measurement system.

As far as the evaluation of $U_I = -2\mathrm{Re}\{Y_d Z\}$ is concerned, we have to observe that, as a result of the definition, the input admittance of each amplifier is equal to $1/Z = j\omega C_{it} + (G_f + j\omega C_f)[1 + \omega_A/(\omega_0 + j\omega)]$, being A_0, ω_0, and ω_A the amplification, the pole frequency, and the gain-bandwidth product of the OPAMP, respectively, while $C_{it} = C_{in} + C_s$ is the total input capacitance of the OPAMP.

Since $|\omega_A/(\omega_0 + j\omega)| \gg 1$, for $\omega \ll \omega_A$, from the expression for $1/Z$ (where $G_s = 0$), one can obtain

$$|U_I| = \frac{2(\omega^2 + \omega_0^2)\left\{G_d(\omega_0 G_f + \omega^2 C_f) + \omega^2 C_d\left[\omega_0 C_f - G_f + \frac{C_{it}}{\omega_A}(\omega^2 + \omega_0^2)\right]\right\}}{\omega_A\left\{(\omega_0 G_f + \omega^2 C_f)^2 + \omega^2\left[\omega_0 C_f - G_f + \frac{C_{it}}{\omega_A}(\omega^2 + \omega_0^2)\right]^2\right\}}, \quad (26)$$

with $|U_I(0)| = 2G_d/(A_0 G_f)$ and $|U_I(\infty)| = 2C_d/C_{it}$.

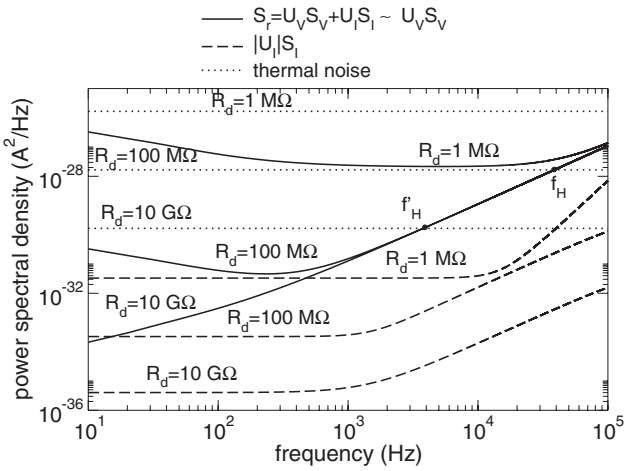

FIG. 5. Plot of $U_V S_V$, $|U_I|S_I$ as a function of frequency, as well as of $S_r = U_I S_I + U_V S_V \approx U_V S_V$ representing the residual noise of the correlated sources, for some values of R_d and for $R_f/R_d = 1$. The upper band limit $f_H = \omega_H/(2\pi)$, as defined in Eq. (27), is shown for $R_d = 100\,\mathrm{M\Omega}$ (f_H) and $R_d = 10\,\mathrm{G\Omega}$ (f'_H).

The noise sources S_V and S_I in Eq. (24) include S_{I_n} and S_{V_n} of the OPAMP, which, for the experimental data that we will report in the following, is a dual TLC072 with a power supply of ± 5 V.

From the datasheet, $S_{I_n} = 3.6 \times 10^{-31}$ A^2/Hz, at 1 kHz, which we assume to be independent of ω (an acceptable approximation in an intermediate frequency range, above the flicker noise corner and below the corner associated with effects due to the input capacitance), while $S_{V_n} = S_{V_0} + S'_{V_n}(\omega)$, where $S_{V_0} = 4.9 \times 10^{-17}$ V^2/Hz (at 1 kHz) and $S'_{V_n}(\omega)$ provided as a function of ω in graphic form by the manufacturer.

As a consequence, since $S_I = S_{I_n} + S_{I_f}$ and, for $R_f = 1\,\mathrm{G\Omega}$, $S_{I_f} = 4k_BT/R_f = 16.6 \times 10^{-30}\,\mathrm{A^2/Hz}$ (T and k_B being the absolute temperature and the Boltzmann constant, respectively), we obtain $S_I \simeq S_{I_f}$. This is *a fortiori* true for $R_f < 1\,\mathrm{G\Omega}$.

With respect to these values and considering also $A_0 = 10^6$, $f_0 = \omega_0/(2\pi) = 10\,\mathrm{Hz}$, $R_{in} = 1000\,\mathrm{G\Omega}$, $C_{in} = 22.9\,\mathrm{pF}$ for the OPAMP, $C_d \simeq C_f \simeq 1\,\mathrm{pF}$, and $C_s = 25\,\mathrm{pF}$, in Fig. 5 we show $U_V S_V$, $U_I S_I$ as a function of f, as well as $S_r = U_I S_I + U_V S_V \simeq U_V S_V$ associated to the residual noise due to the correlated sources, for some choices of R_d and for $R_f/R_d = 1$; in the same figure we also plot the thermal noise of R_d, $S_{I_d} = 4k_BTG_d$, which represents the quantity of interest to be measured in this example.

For large values of f, we have $S_r = U_V S_{V_0} = 2C_dC_p\omega^2 S_{V_0}$, yielding the upper band limit ω_H, defined by the condition $S_r(\omega_H) = S_{I_d}$, in the form

$$\omega_H = \left(\frac{S_{I_d}}{2C_dC_pS_{V_0}}\right)^{1/2}, \tag{27}$$

while the lower band limit ω_L, for $S_r(\omega_L) = S_{Id}$, can be numerically evaluated.

However, in an actual measurement, performed with a DSA, we do not get the ideal value of the cross-power spectral density but an estimate of it, which is evaluated by performing averages of $Q_1Q_2^*$,[9,10] where Q_1 and Q_2 are the Discrete Fourier Transforms (DFT) of the time records over an interval τ of the quantities $q_1(t)$ and $q_2(t)$, respectively. More precisely, since we are working in terms of power spectral densities, the cross-power spectral density obtained by the DSA corresponds to $\langle Q_1Q_2^*\rangle/(\Delta f)$, where a normalization for the DFTs has been chosen such that they are expressed in the same units as the initial quantities q_1 and q_2, and Δf is the frequency resolution, i.e., $1/(N\tau)$ (N being the number of samples in the time record and τ the sampling interval). This implies that for a finite number of averages the estimate of the cross-power spectral density will include, beyond the terms in Eq. (23), also a term S_u resulting from the variance of the estimate of the uncorrelated contributions around the null mean value.

An estimate of S_u from the acquisition of a single time series can be obtained from Eqs. (9) and (19), considering that $|Z_k| \ll |Z_d|$:

$$S_u \approx 2\sqrt{S_{I_d}}\sqrt{S_I} + S_I + 2(\sqrt{S_{I_d}} + \sqrt{S_I})\sqrt{S_V}(|Y_p| + |Y_d|) + S_V(|Y_p|^2 + |Y_d|^2), \tag{28}$$

where S_{I_d} is the noise power spectral density of the DUT, S_I that associated with the I_js (which in most cases can be approximated with just the contribution of the feedback resistor, $4k_BT/R_f$), S_V is that of the noise input voltage sources V_j. As far as the admittances are concerned, $Y_d = 1/R_d + j\omega C_d$ and $Y_p = 1/R_d + 1/R_f + j\omega(C_d + C_s + C_d) = 1/R_d + 1/R_f + j\omega C_p$, since Z_s is assumed to be purely capacitive.

The actual magnitude of the estimate of the uncorrelated component resulting from the averaging procedure will depend on the number of averages (theoretically it would drop to zero after averaging over an infinite number of time records). A reliable approximation of its standard deviation is obtained[10–12] dividing S_u by the square root of the number of averages M. If only the real part of the measured cross-power spectral density is considered, the result is further divided[1,11,12] by $\sqrt{2}$, thus obtaining $S_u/\sqrt{2M}$, which thus represents the standard deviation of the uncorrelated residual after M averages.

When the standard deviation of the estimate of the uncorrelated residual $S_u/\sqrt{2M}$ equals the correlated residual S_r any further increase in the number of averages can at most further reduce the noise floor by a factor of 2. Thus, we can consider the number of averages for which this equality is verified as the maximum number of averages that is meaningful to perform.

Such a number can be easily deduced from a comparison of the plots of S_u and of S_r (see Fig. 6): if they are represented in a logarithmic scale the distance between the curves corresponds to the logarithm of their ratio, therefore to $\log\sqrt{2M}$. In Fig. 6, we report plots of S_r, S_u, and thermal noise, as a function of R_d for three different frequency values and for two choices of the ratio R_f/R_d: 1 (upper curves) and 10 (lower curves). Moreover, the dots on the plot of S_r indicate the maximum value of R_d for which thermal noise measurements are possible.

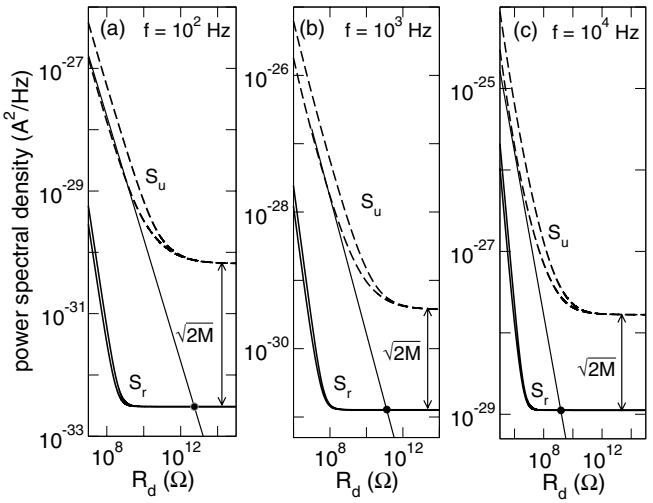

FIG. 6. Plot of S_r (thick solid line), S_u (dashed line), and thermal noise of R_d (thin solid line) as a function of R_d, computed for three frequency values and for R_f/R_d=1 (upper curves) and R_f/R_d=10 (lower curves). The distance between the curves S_u and S_r corresponds to the logarithm of $\sqrt{2M}$, with M being the number of averages needed to make the standard deviation of the estimate of the uncorrelated component in the cross-power spectral density equal to the residual unwanted correlated component. The dots on the plot of S_r indicate the maximum value R_{dM} of R_d for which its thermal noise is greater or equal to S_r itself. From Eq. (24), in which $U_I S_I$ is negligible (see Fig. 5), for $R_d \to \infty$ we have $S_r = 4k_BT/R_d$ for $R_{dM} = 2k_BT/(C_pC_d\omega^2 S_V)$ whereas, for $R_d \to 0$, we have $S_r = 4k_BT/R_d$ for the minimum value $R_{dm} = (1 + R_d/R_f)S_V/(2k_BT)$. In the range R_{dm}, R_{dM} thermal noise measurements on R_d are possible.

Thus, since the time to acquire a single time record is known, from the number of averages M required to achieve the desired sensitivity it is possible to compute the expected duration of the measurement.

IV. AMPLIFIERS CONNECTED IN PARALLEL

When R_d is smaller than the optimal resistance $\sqrt{S_{V_n}/S_{I_n}}$ of the amplifier, the effect of the input equivalent voltage noise sources becomes prevalent with respect to that due to the input equivalent noise current sources, and thus in the series two-channel system the residual noise increases with decreasing R_d, since the contribution of the voltage noise sources is not significantly suppressed in such a correlation scheme [see Eqs. (24) and (25), and Fig. 6].

As a consequence, it is preferable to adopt a different solution, such as, for example, the one in Fig. 2, in which the noise voltage of the DUT is measured using the two voltage amplifiers in parallel, with the correlation technique suppressing, this time, the effects of the uncorrelated noise voltages sources.

The bias voltage V_P is useful to remove the DC component at the output [e.g., $V_D(1 + R_1/R_2)$], which otherwise would have a nonzero value due to the bias applied to the DUT.

Also in this case, V_s, T_0, and Z_s are used for the measurement of the transimpedance between I_d and the outputs.

The system allows to directly measure S_{I_d}, from which one can obtain $S_{V_d} = |Z_d|^2 S_{I_d}$, once Z_d is known.

Let us first determine the equivalent input noise sources of the noninverting amplifiers: with reference to Fig. 7(a), we should take into consideration the voltage and current noise sources at the input of the operational amplifier and the thermal noise sources associated with R_1 and R_2. Let us proceed in a way analogous to what we have done for the determination of the equivalent input noise sources in the case of the series configuration. From the comparison of Figs. 7(a) and 7(b), we obtain that the power spectral density of the equivalent input voltage noise source V_n' is given by

$$S_{V_n'} \simeq S_{V_n} + 4k_BTR_1, \tag{29}$$

in the hypothesis that R_1 has been chosen such that $R_2 \gg R_1$ and $S_{V_n}/S_{I_n^-} \gg R_1^2$. These inequalities are in general satisfied if we have amplifiers with a large enough gain and R_1 is selected small enough, on the basis of the values of the equivalent input equivalent noise power spectral densities of the amplifier. We also obtain that $S_{I_n'} \simeq S_{I_n^+}$ if $A_v R_1/R_2 \gg 1$ and $R_2 \gg R_1$. Moreover, in Fig. 8(b) $A_j = 1 + R_2/R_1$ and $Z_{ij} = (1 + A_v/A_j)Z_{in} + R_2/A_j$ are the gain and the input impedance, respectively, of the noninverting voltage amplifier.

In Fig. 8, the resulting equivalent circuit for the evaluation of V_{oj} is shown, in which

$$I = I_{n1}' + I_{n2}' + I_b + I_s + \frac{V_s}{Z_s}, \tag{30}$$

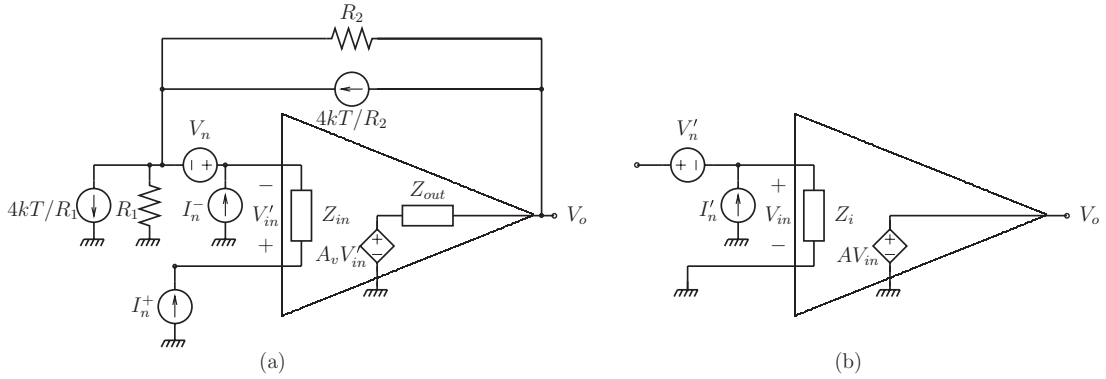

FIG. 7. (a) Noninverting voltage amplifier used for the parallel configuration, with the indication of all noise sources; (b) equivalent circuit for the noninverting amplifier with equivalent voltage and current noise sources at the input.

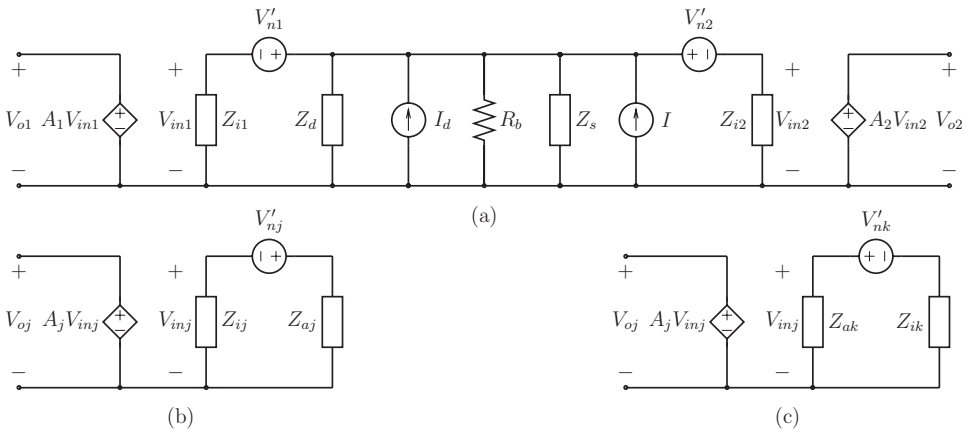

FIG. 8. (a) Equivalent circuit of the measurement system of Fig. 2; (b) and (c) equivalent circuits for the evaluation of the contribution to V_{inj} of V'_{nj} and of V'_{nk}, respectively.

where $V_s = 0$ for T_0 in position 1, $I'_{nj} = I^+_{nj}$, I_b and I_s are the equivalent current noise sources of the impedances R_b and Z_s, respectively.

The expression of the voltage V^I_{oj} due to the current noise source reads

$$V^I_{oj} = (I + I_d)Z_t A_j, \tag{31}$$

where I_d is the noise current source of the DUT and $Z_t = Z_d \parallel R_b \parallel Z_s \parallel Z_{i_1} \parallel Z_{i_2}$ is the total parallel impedance seen by I_d.

If V_s, when T_0 is in position 2, yields a signal that is much larger than that of the equivalent noise sources, from Eq. (31) we obtain $\hat{V}^I_{oj} = H_j V_s$, where

$$H_j \equiv \frac{Z_t}{Z_s} A_j \tag{32}$$

is the amplification between V_s and V_{oj}.

In Figs. 8(b) and 8(c), we show the circuit for the evaluation of V^V_{oj} due to V_{nj} and V_{nk}, where $Z_{aj} = Z_{ik} \parallel R_b \parallel Z_d \parallel Z_s$ is the impedance at the input of jth noninverting amplifier, so that we have also $Z_t = Z_{ij}Z_{aj}/(Z_{ij} + Z_{aj})$ and

$$V^V_{oj} = \left(-\frac{V'_{nj}}{Z_{aj}} + \frac{V'_{nk}}{Z_{ik}}\right) A_j Z_t. \tag{33}$$

Finally, from Eqs. (31) and (33), the equivalent noise current source $I_{ej} \equiv V_{oj}/A_j Z_t$ reads

$$I_{ej} \equiv \frac{V_{oj}}{A_j Z_t} = I_d + I - \frac{V'_{nj}}{Z_{aj}} + \frac{V'_{nk}}{Z_{ik}}, \tag{34}$$

where $V_{oj} = V^I_{oj} + V^V_{oj}$ is the total voltage measured at the output j. From Eqs. (32) and (34) we obtain

$$S_{I12} \equiv \frac{S_{12}}{|Z_s|^2 H_1 H_2^*} = S_{I_d} + S_I - \frac{S_{V_1}}{Z^*_{i1} Z_{a1}} - \frac{S_{V_2}}{Z_{i2} Z^*_{a2}}, \tag{35}$$

$$S_{I11} \equiv \frac{S_{11}}{|Z_s H_1|^2} = S_{I_d} + S_I + \frac{S_{V_1}}{|Z_{a1}|^2} + \frac{S_{V_2}}{|Z_{i2}|^2}, \tag{36}$$

where S_{12} (S_{11}) is the measured cross-power spectral density (power spectral density) at the outputs and S_I is the power spectral density of I. From Eqs. (35) and (36) we observe that cross-correlation reduces the effect of V_{nj} at low frequency by a factor of $G_a/G_i \to \infty$, being $G_a = \mathrm{Re}\{1/Z_d\}$ and $G_i = \mathrm{Re}\{1/Z_i\} \simeq 0$ for voltage amplifiers.

When $G_i = 0$, from Eq. (35) we obtain again Eq. (23), and the residual of the correlation S_r reads, for equal channels,

$$S_r = S_I - 2C_i C_a \omega^2 S_V, \tag{37}$$

where $S_V \equiv S_{V'_{n1}} = S_{V'_{n2}}$ and, for $Z_s = 1/j\omega C_s$, $S_I = 2S_{In} + 4k_B T/R_b$; C_a is the capacitance associated with Z_a.

In Fig. 9, $|S_r|$, S_{I_d}, and $|S_{I_d} + S_r|$ are plotted as a function of f. Since, at high frequencies, from Eq. (37) it is $|S_r| \simeq 2C_{in}C_a\omega^2 S_V$, the upper frequency limit ω_H defined by $|S_r(\omega_H)| = S_{I_d}$ reads

$$\omega_H = \left(\frac{S_{I_d}}{2C_i C_a S_V}\right)^{1/2}, \tag{38}$$

similar to Eq. (27), whereas ω_L can be obtained graphically from the data for S_{I_n} provided by the manufacturer of the amplifier.

When evaluating S_{I12} according to Eq. (35), but with no averages, we have to take into account the cross products of

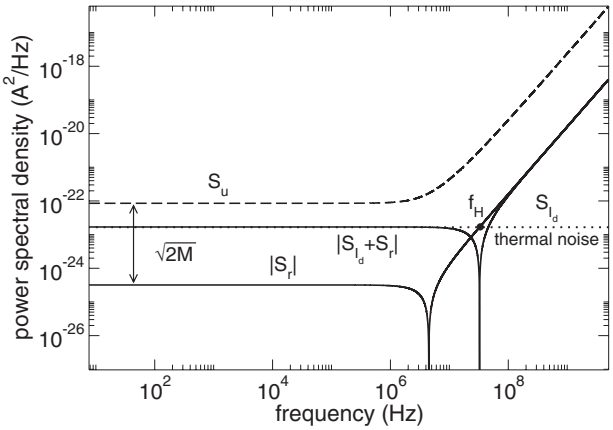

FIG. 9. Plot of $|S_{I_d} + S_r|$, $|S_r|$, and S_u as a function of frequency for $R_d = 1\,\mathrm{k}\Omega$. The distance between the curves S_u and $|S_r|$ corresponds to the logarithm of $\sqrt{2M}$, with M being the number of averages needed to make the standard deviation of the estimate of the uncorrelated component in the cross-power spectral density equal to the residual unwanted correlated component.

the uncorrelated quantities V_{nj}, I_{nj}, and I_d. From Eqs. (30) and (34), considering the impedance Z_s as noiseless, and remembering that $|Z_{ij}| \gg |Z_{aj}|$, an estimate of S_u reads

$$S_u = 4\sqrt{S_{I_d}}\sqrt{S_{I_n'}} + 2\sqrt{S_{I_d}}\sqrt{S_{I_b}} + 2S_I + 4\sqrt{S_{I_n'}}\sqrt{S_{I_b}} + 2(\sqrt{S_{I_d}} + 2\sqrt{S_{I_n'}} + \sqrt{S_{I_b}})\sqrt{S_V}|Y_a| + S_V|Y_a|^2, \tag{39}$$

where we have considered identical channels and thus $Z_{a1} = Z_{a2} = 1/Y_a$.

We have computed S_u for the particular case in which the operational amplifier is an OP27 (suitable for operation with low to medium impedance sources), characterized by an equivalent input noise voltage power spectral density of 9×10^{-18} V^2/Hz and an equivalent input noise current power spectral density of 0.16×10^{-24} A^2/Hz. The resistors are assumed to be $R_1 = 1$ kΩ and $R_2 = 1$ MΩ, which satisfies the previously mentioned conditions $R_2 \gg R_1$ and $S_{V_j}/S_{I_n^-} \gg R_1^2$.

The plot of the thus computed estimate of S_u is reported in Fig. 9 along with that of $|S_r|$, in a logarithmic scale, and, at frequencies for which $S_r > 0$, their difference corresponds to the logarithm of $\sqrt{2M}$, with M being the number of averages needed to make the standard deviation of the uncorrelated contribution to the estimate of the cross-power spectral density comparable to the residual correlated term S_r. For the evaluation of S_u we have considered the previously discussed typical parameters for the low-noise operational amplifier OP27.

V. EXPERIMENTAL RESULTS AND DISCUSSION

In this section, we report the results of measurements that we have performed to validate our theoretical conclusions. Measurements have been performed on resistors (RNX series by Dale-Vishay) kept at room temperature (acquired with a thermometer in direct contact with them), so that their thermal noise could be computed exactly and could thus be compared with the outcome of the experiments. We have first performed tests on the "series" configuration, using a dual operational amplifier TLC072, and, for the impedance Z_s, a 75 pF capacitor.

In Fig. 10, we show $S_{I_d}(\omega)$ for $R_d = R_f = 100$ MΩ, operating with only one (curves (a) and (b)) or with both (curves (c) and (d)) channels and the correlation procedure for the reduction of the residual uncorrelated noise. In particular, curves (a) and (c) refer to results obtained without applying our procedure for the measurement of the transimpedance (using simply an estimate based on the characteristics of the amplifier and the values of the components at low frequencies), while curves (b) and (d) report results obtained with the application of our method for the evaluation of the transimpedance.

In Fig. 11, the measured noise power spectral density (solid line) is also compared with that (dotted line) computed by means of Eq. (23). The upper band limit $f_H \simeq 9$ kHz that can be deduced from this plot is substantially coincident with the one calculated from Eq. (27) for $C_s = 75$ pF, $C_d = 6.5$ pF,

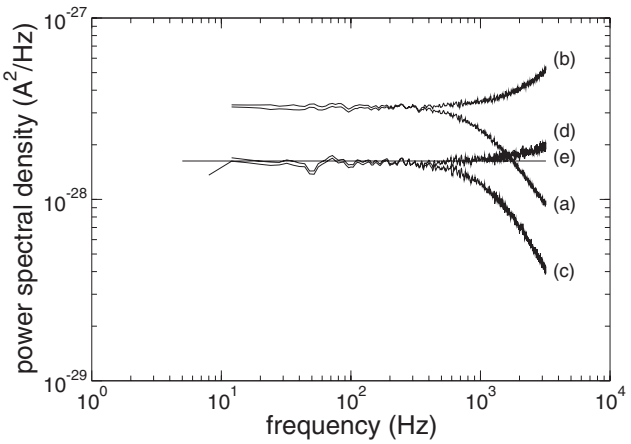

FIG. 10. Noise current power spectral density as a function of frequency for a resistor $R_d = 100$ MΩ, measured with a single ((a) and (b)) transimpedance amplifier ($R_f = R_d$) and with the correlation amplifier ((c) and (d)); the solid line (e) represents the ideal value $4k_BT/R_d$. Plots (b) and (d) [(a) and (c)] are obtained by means of [without] the method for the evaluation of the transimpedance.

$C_f = 1$ pF. The dashed line corresponds to the expected thermal noise $4k_BTG(f)$, where $G(f)$ is the measured real part of the parallel equivalent representation, in terms of admittance, of the resistor. There is an increase in the upper frequency range, due to the presence of distributed capacitance.

In Fig. 12, we report the measured and computed noise power spectral density for a few values of R_d. The detailed dependence on frequency of the equivalent input noise sources of the operational amplifiers has been included, and a good agreement is achieved, even at low frequencies and for small values of R_d, where also flicker noise contributions produce a nonnegligible effect. We have included the measured dependence on frequency of the real part of the conductance for the parallel representation of R_d, which, in the frequency range of interest, exhibits significant deviations from a constant value only for the 100 MΩ and 1 GΩ cases (the parallel conductance of the 100 MΩ resistor increases by 2% at 10 kHz, while

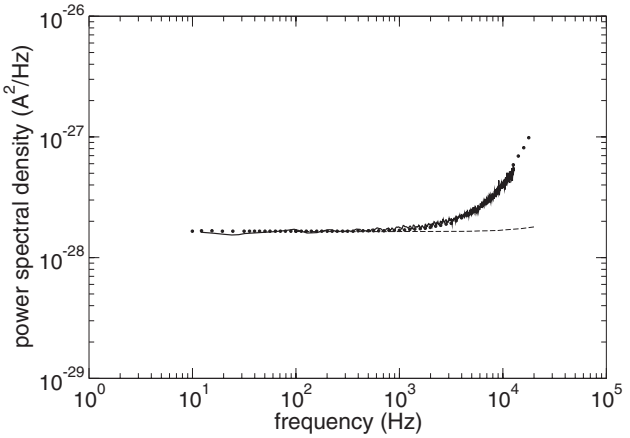

FIG. 11. Comparison between the noise current power spectral density as a function of frequency for a resistor $R_d = 100$ MΩ, measured with the correlation amplifier (solid line) and the value calculated by means of the model proposed in this paper (dotted line). The dashed line represents the ideal value $4k_BTG(f)$, where $G(f)$ is the conductance in the parallel equivalent representation of R_d.

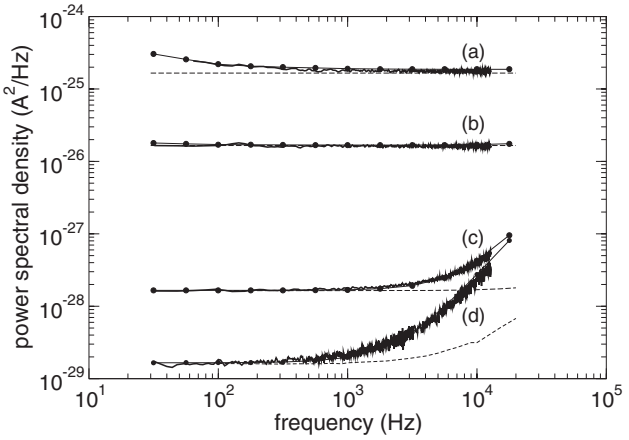

FIG. 12. Measured current noise power spectral density (solid line) for the series configuration and values of the resistance $R_d = 100\,\text{k}\Omega$ (a), $R_d = 1\,\text{M}\Omega$ (b), $R_d = 100\,\text{M}\Omega$ (c), $R_d = 1\,\text{G}\Omega$ (d) at room temperature, in comparison with the ideal expected value $4k_BTG(f)$ (dashed line) and the value obtained from the model proposed in this paper (dotted line).

that of the 1 GΩ resistor increases by about 80% at the same frequency.

From the comparison of the obtained numerical and experimental results with the actual power spectral density, the increase in sensitivity and accuracy afforded by the proposed method is apparent. In more challenging measurement conditions, when the noise of the DUT is even further below the noise floor of the amplifier, a proper evaluation of the transimpedance becomes more important, affecting the outcome of the measurement at all frequencies.

The results presented so far are for relatively large values of the DUT differential resistance, for which the series configuration of the amplifiers is preferable. As the DUT resistance is decreased, the parallel configuration becomes more suitable, and we have performed experimental tests that include also this case.

In Fig. 13, we present a combination of results for the series and the parallel configuration. We plot the measured noise current power spectral density as a function of R_d, in the range between 10 Ω and 1 GΩ, with the purpose of evaluating the deviation from the exact value (solid line). For values of R_d above 100 kΩ the measurement has been performed with the series (transimpedance) configuration (with $R_f = 10\,\text{M}\Omega$), while below 100 kΩ the parallel (voltage) configuration has been adopted, using commercial EG&G 5003 amplifiers (instead of the noninverting configuration with OP27 operational amplifiers that we have previously considered). The circular dots represent the results obtained with the application of our method, while the triangles correspond to the results measured with a single amplifier: it is apparent that our method is most advantageous in the critical regions of very large or very small differential resistance, where the current or voltage noise sources, respectively, become prevalent and their contributions can be suppressed with the correlation procedure, while the precise evaluation of the transimpedance helps in improving the accuracy of the final result.

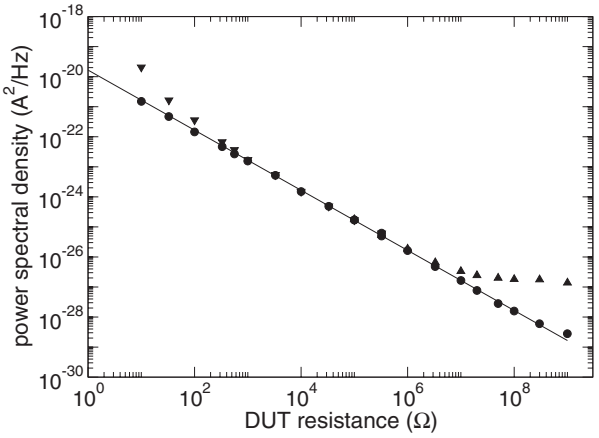

FIG. 13. Noise current power spectral density (dots) measured with the correlation amplifier in the series ($R_d > 100$ kΩ) and the parallel ($R_d < 100\,\text{k}\Omega$) configuration, compared with the ideal value (solid line); the triangles show the results that would have been obtained with a single voltage ($R_d < 100\,\text{k}\Omega$) or transimpedance ($R_d > 100\,\text{k}\Omega$) amplifier.

The contribution of the transimpedance evaluation is even more relevant in the case of nonlinear DUTs, for which the differential resistance of the DUT has a strong dependence on the operating point, and therefore must be evaluated with the very same bias applied during the noise measurement. It has been our experience that in the case, for example, of *p-n* junctions the small errors resulting from the evaluation of the differential resistance from the $I - V$ characteristic (via numerical derivation) or via a direct measurement with an impedance meter may lead to quite significant errors in the resulting estimate of the noise power spectral density.

However, since for the application of the transimpedance method we need to include a capacitor C_s that during the noise measurement will be in parallel to the input of the amplifiers, the improved accuracy is obtained, according to Eq. (27), at the expense of the bandwidth, with a reduction of f_H by about a factor of $[1 + C_s/(C_s + C_d)]^{1/2}$.

The proposed set-up and method have been applied, in particular, to the measurement of shot noise in quasi-ideal and in commercial silicon and gallium arsenide *p-n* junctions over 4 decades of bias current, down to 10 pA.[13] The experimental results show for the first time a V-shaped behavior of the Fano factor, in agreement with a theoretical model that explains it on the basis of the carrier generation-recombination in the junction depletion layer. Such an achievement would not have been possible without the accuracy and sensitivity of the proposed measurement technique.

Furthermore, with cryogenic cooling at a temperature of about 6 K of the feedback resistors, we have been able, with the usage of the series configuration, to reliably measure the shot noise of resonant tunneling diodes associated with a current down to a fraction of a picoampere.[14]

VI. CONCLUSIONS

We have presented a detailed analysis of correlation techniques for noise measurements, coupled with a procedure that allows the precise evaluation of the transfer function between the noise source and the amplifier outputs, an issue that is often overlooked, even in the recent literature on noise

characterization. We provide an analytical treatment, with expressions for the evaluation of the actual noise power spectral density of the device under measurement and the estimation of the residual background terms, as a function of the number of averages. These relationships can also be used to determine the number of averages that need to be performed to achieve a given accuracy.

Both the "series" and "parallel" configurations for correlation measurements have been taken into consideration, and criteria for the choice between them have been discussed. The theoretical results have been validated by means of measurements on resistors with known noise behavior.

Our technique has been successfully applied to particularly challenging shot noise measurements, on strongly nonlinear devices. It has made possible the precise evaluation of the noise power spectral density of *p-n* junctions over several decades of bias current, starting from a value of about 10 pA, thereby achieving for the first time a complete experimental characterization of shot noise suppression due to generation-recombination effects. It has also enabled us to reliably and routinely measure, if cryogenic cooling of the feedback resistors is used, the shot noise in double barrier resonant tunneling devices due to currents below 1 pA.

[1]M. Sampietro, L. Fasoli, and G. Ferrari, Rev. Sci. Instrum. **70**, 2520 (1999).
[2]G. Ferrari and M. Sampietro, Rev. Sci. Instrum. **73**, 2717 (2002).
[3]L. DiCarlo, Y. Zhang, D. T. McClure, and C. M. Marcus, Rev. Sci. Instrum. **77**, 073906 (2006).
[4]F. Crupi, G. Giusi, C. Ciofi, and C. Pace, IEEE Trans. Instrum. Meas. **55**, 1143 (2006).
[5]G. Giusi, F. Crupi, C. Ciofi, and C. Pace, Rev. Sci. Instrum. **77**, 095104 (2006).
[6]G. Giusi, F. Crupi, C. Ciofi, and C. Pace, Rev. Sci. Instrum. **77**, 015107 (2006).
[7]G. Giusi, C. Pace, and F. Crupi, Int. J. Circuit Theory Appl. **37**, 781 (2009).
[8]M. Macucci and B. Pellegrini, IEEE Trans. Instrum. Meas. **40**, 7 (1991).
[9]C. W. Therrien, *Discrete Random Signals and Statistical Signal Processing* (Prentice Hall, Englewood Cliffs, NJ, 1992), p. 657.
[10]P. D. Welch, IEEE Trans. Audio Electroacoust. **AU-15**, 70 (1967).
[11]G. M. Jenkins and D. G. Watts, *Spectral Analysis and Its Applications* (Holden-Day, Oakland, CA, 1968).
[12]G. M. Jenkins, in *Proceedings of the Symposium on Time Series Analysis*, edited by M. Rosenblatt (John Wiley, New York, 1963), p. 267.
[13]I. A. Maione, B. Pellegrini, G. Fiori, M. Macucci, L. Guidi, and G. Basso, Phys. Rev. B **83**, 155309 (2011).
[14]I. A. Maione, M. Macucci, G. Iannaccone, G. Basso, B. Pellegrini, M. Lazzarino, L. Sorba, and F. Beltram, Phys. Rev. B **75**, 125327 (2007).